JOURNAL OF CATALYSIS 128, 231–247 (1991)

The Role of Surface Structure and Dispersion in CO Hydrogenation on Cobalt

BYRON G. JOHNSON,* CALVIN H. BARTHOLOMEW,* AND D. WAYNE GOODMAN†

*BYU Catalysis Laboratory, Department of Chemical Engineering, Brigham Young University, Provo, Utah 84602; and †Department of Chemistry, Texas A&M University, College Station, Texas 77843

Received August 7, 1989; revised September 17, 1990

The effects of surface structure on the CO hydrogenation reaction have been investigated by comparing the steady-state activity and selectivity of submonolayer cobalt deposited on W(110) and W(100) with those of carbonyl-derived Co/alumina catalysts of varying dispersion and extent of reduction. The Co/W surfaces have highly strained and different geometries (*1*) but have similar activity. The activity matches that of the highly active, highly reduced Co/alumina catalysts, suggesting that the steady-state activity of cobalt surfaces is independent of surface structure. AES spectra show the after-reaction Co/W surfaces to have high coverages of both carbon and oxygen, with carbon lineshapes characteristic of carbidic carbon. Carbonyl-derived Co/dehydroxylated alumina catalysts have high extents of reduction, high dispersions, and good activity stability. Increasing the dehydroxylation temperature of the alumina support increases metal dispersion while decreasing CO_2 and olefin selectivities. Specific CO hydrogenation activity is constant over the range of dispersion of 5–37% for highly reduced 3 and 5% Co/alumina catalysts and over the entire range of dispersion (0–100%) if polycrystalline Co and Co/W surfaces are included. The specific activity of carbonyl-derived catalysts appears to be more closely related to the extent of reduction and the support dehydroxylation temperature than to the dispersion. Thus, the chemical nature of the support surface appears to be the controlling factor in determining the specific activity of supported cobalt catalysts.

INTRODUCTION

Activities and selectivities of supported CO hydrogenation catalysts vary substantially with the metal loading, preparation method, and type of support (*2–8*). Specific activities of supported Ru (*3*), Co (*4, 5*), Fe (*2, 6, 7*), and Ni (*8*) decrease 1–2 orders of magnitude with increasing dispersion. Several authors (*2, 3, 5*) have suggested that these changes in activity may result from changes in the particle size (or dispersion) of the active metal phase. Since the surface structure of supported metals varies with the dispersion (*9*), CO hydrogenation on these metals appears as if it might be structure sensitive (*2*).

The structure sensitivity of reactions can be confirmed by performing high-pressure reaction studies on metal single crystals (*10*). For example, ammonia synthesis activity varies over 2 orders of magnitude on Fe(111), Fe(100), and Fe(110) (*11*). Also, Ni(111) and Ni(100) are clearly different in activity and activation energy for the ethane hydrogenolysis reaction (*12*). However, surface science studies suggest that CO hydrogenation on Group VIII metals is structure *insensitive*. For example, the methanation rate of Ni(111) is identical to that of Ni(100), and their activities compare very well with those of several supported nickel catalysts (*13*). Similar results are observed for methanation on Ru(001) and Ru(110) (*14*). While the ethane hydrogenolysis rate increases with the increasing geometric strain of nickel overlayers on W(110) and W(100), the CO hydrogenation rate is independent of structure and Ni coverage (*15*).

Explanations proposed for the observed specific activity changes of supported catalysts with metal loading and dispersion in-

0021-9517/91 $3.00

clude primary structure sensitivity, secondary structure sensitivity, and metal-support interactions.

Primary structure sensitivity implies that planer (high coordination) surface sites are intrinsically more active than edge and corner (low coordination) sites (*3*). However, this hypothesis is not consistent with the previously mentioned surface science studies of CO hydrogenation.

Secondary structure sensitivity (*16*) results from selective self-poisoning mechanisms. CO dissociation is favored on low coordination sites (*17–21*). Schmidt and coworkers (*22, 23*) have shown selective poisoning of low-coordination sites by graphite on a curved nickel single crystal. Kelley and Goodman (*13*) have shown that the specific activity of Ni(100) decreases 2 orders of magnitude with increasing surface carbide level. The greater abundance of low-coordination sites on highly dispersed catalysts could increase CO dissociation, thereby increasing the surface carbide level or causing graphite formation, and thus decrease the specific activity of the catalyst.

Metal-support interactions involve several kinds of chemical/physical phenomena and are more pronounced in highly dispersed catalysts (*24*). A number of studies (*24*) show that hydrogen adsorption kinetics and energetics are affected by decoration of small metal crystallites by support moieties. Recent temperature-programmed surface reaction (TPSR) studies (*25–27*) have shown that there are two sites or reaction states for CO hydrogenation on supported metal catalysts. In the case of Co/Al_2O_3 and Ni/Al_2O_3, the less active of these states may be a reaction involving decomposition of a species formed on the support (*25*). The relative abundance of the less active state decreases with increasing metal loading. Studies of Bartholomew *et al.* (*6, 28, 29*) also provide evidence that the adsorption, activity, and electronic properties of tiny metal clusters in 1–3% Co/Al_2O_3, Fe/Al_2O_3, and Fe/C systems are substantially altered due to direct interaction with and/or decoration by the support. For example, CO does not adsorb dissociatively on 1% Co/Al_2O_3 at 400–600 K while it clearly dissociates on 3–25% Co/Al_2O_3 under the same conditions (*28*). Thus, while metal-support interactions involve varied and complex phenomena, they might explain the observed variations in activity and selectivity of supported Group VIII metals with dispersion, metal loading, and preparation method (*30*).

The objective of this study was to determine the cause of the observed activity variations in supported cobalt catalysts with metal loading and dispersion (*4, 5*), using a combined, systematic surface science/reaction study of Co/W surfaces and supported cobalt catalysts. The CO hydrogenation activity and selectivity of submonolayer Co/W(110) and Co/W(100) surfaces were determined at steady state and under realistic pressure conditions (750 Torr). The after-reaction surface coverages of carbon and oxygen were analyzed by Auger electron spectroscopy (AES). A series of cobalt/alumina catalysts of varying dispersions were prepared by decomposing tetracobalt dodecacarbonyl on dehydroxylated alumina supports, and then tested for CO hydrogenation activity and selectivity at 1 atm.

We have recently published a study on the structural and chemisorptive properties of ultrathin cobalt overlayers on W(110) and W(100) (*1*). The Co/W system was chosen because of the difficulty involved in cleaning cobalt single crystals (*31*) and the success found in preparing clean, pseudomorphic metal overlayers on tungsten single crystals (*32–34*). Cobalt was found to form pseudomorphic monolayers on W(110) and W(100) which are thermally stable to 1300 K. The monolayers take on the geometry of the tungsten substrate, and are thus geometrically strained with respect to bulk cobalt surfaces. Accordingly, these surfaces provide wide variations in the cobalt surface structure. Due to electronic interactions with the tungsten, the cobalt monolayers

have enhanced CO dissociation ability. The cobalt overlayers also have high-temperature hydrogen adsorption states.

Conventional supported cobalt catalysts are typically prepared by aqueous impregnation of cobalt (II) salts, drying or calcination to produce cobalt oxide precursors, and finally reduction in hydrogen (*35*). Because of strong interaction with the oxidic support, these oxide precursors are quite difficult to reduce. Catalysts prepared using metal carbonyls as precursors have been found to have higher extents of reduction and higher dispersions (*36–38*). In preparing carbonyl-derived catalysts it is important to dehydroxylate the alumina support prior to introduction of the metal carbonyl. This avoids oxidation of the metal during subsequent carbonyl decomposition (*36–38*).

EXPERIMENTAL

Co/W Single Crystals

Apparatus. The single crystal experiments were performed in a previously described (*15, 39*) specialized apparatus which links a high-pressure, batch catalytic reactor with a UHV surface analysis chamber. Both regions were capable of achieving base pressures of 1×10^{-10} Torr. Tungsten single crystal samples were mounted on a retraction bellows, which allows *in vacuo* translation between the chambers. The surface analysis chamber was equipped with a single pass cylindrical mirror analyzer for Auger electron spectroscopy (AES), and a cobalt source for vapor-depositing cobalt onto the tungsten crystals. The cobalt source was a resistively heated 0.25-mm tungsten filament wrapped with 99.997%, 0.25-mm cobalt wire. The cobalt source was extensively outgassed in vacuum to deplete the bulk of impurities. The reaction chamber could be isolated from the surface analysis chamber with an all-metal-seal gate valve and pressurized to <2 atm. The gas pressure was measured with a capacitance manometer. The reaction chamber was connected to a gas chromatograph through a gas manifold system for direct analysis of reaction products.

Crystal preparation. The W(110) and W(100) crystals were spotwelded to short, high-purity tungsten leads and could be resistively heated up to 1800 K. A W-5%Re/W-26%Re thermocouple was spotwelded to the back edge of the crystal for temperature measurement. An electron beam heater was used to attain temperatures between 1800–2300 K. The W crystals were cleaned by heating in 1×10^{-6} Torr oxygen at 1500 K for 10 min, followed by several annealing cycles (in vacuum at 2300 K for 15 s), until no impurities were detected by AES. Cobalt was dosed onto the front face of the clean tungsten crystals by placing the room temperature crystal in front of the cobalt source until the unannealed Co(775)/W(169) AES ratio corresponded to 0.75 ml coverage of cobalt (*1*). The crystals were then annealed in vacuum at 1100 K for 30 s.

Kinetic testing. The annealed Co/W crystal was isolated in the 0.6-liter batch reaction chamber and high-purity CO was admitted to 250-Torr pressure. The CO stream was purified by passing it through a glass-wool packed trap at liquid nitrogen temperature (to remove impurity carbonyls). High-purity hydrogen was then added until the chamber pressure reached 750 Torr, resulting in a molar H_2/CO ratio of 2. The crystal was then resistively heated to the reaction temperature and held there for 1 h. This long reaction time was used to obtain high enough conversion for product analysis (the crystal had less than 1 cm^2 of Co surface area), and to assure steady-state conditions. Gas products (C_1–C_5) were analyzed by gas chromatography with a flame ionization detector. Response factors were determined using gas mixtures of known concentration. CO conversions were typically much less than 1%. CO_2 selectivities were not obtained. Carbon and oxygen levels on the crystal were then determined in the surface analysis chamber by AES after a 600 K an-

neal under UHV (to remove molecularly adsorbed CO). The kinetic procedure was then repeated at higher temperatures to obtain the Arrhenius behavior. The crystals were not recleaned between kinetic tests. However, the reproducibility of the kinetic measurements indicated a stable surface. Turnover frequencies were determined by calculating the number of surface cobalt sites from the geometric area of the front face of the tungsten crystal, the surface atomic densities of W(110) and W(100), and the coverage of cobalt.

Cobalt/Alumina Catalysts

Catalyst preparation. Conoco DISPAL M γ-Al_2O_3 was calcined at 773 K overnight and then dehydroxylated under vacuum at 923 K (923 DHD) or 1223 K (1223 DHD) for 4 h. $Co_4(CO)_{12}$ and $W(CO)_6$ were obtained from Strem Chemicals. Due to the low solubility of the solid carbonyls, the carbonyl-derived catalysts were prepared by a Soxhlet reflux method. Ten grams of dehydroxylated γ-Al_2O_3 was mixed with 350 ml of cyclohexane and stirred. Enough $Co_4(CO)_{12}$ or $W(CO)_6$ (usually 0.5–2.0 g) to produce the desired weight loading of metal was placed in the Soxhlet paper cup filter, and the system was refluxed at 353 K for 24 h. Excess solvent was poured off and the catalyst samples were dried by evacuation. The catalysts were then reduced in flowing hydrogen at 2000 h^{-1} with a ramp of 5 K/min and a hold for 16 h at 623 K. The carbonyl was expected to completely decompose during this reduction treatment (*40*). Catalyst preparation, handling, and storage were all performed under inert atmosphere in a glove box or vacuum system to avoid oxidation of the cobalt and tungsten. The cobalt and tungsten loadings of the catalysts were determined (after reduction and oxygen titration) by chemical analysis using atomic absorption spectroscopy.

Chemisorption measurements. Hydrogen chemisorption was performed statically on 1 g of reduced catalyst in a Pyrex volumetric adsorption apparatus. Since hydrogen adsorption on cobalt is an activated process (*35*), the hydrogen isotherms were obtained after adsorbing a measured quantity of hydrogen at 623 K and then cooling to room temperature. Extents of reduction were determined by oxygen titration at 673 K, where the reaction of reduced cobalt with oxygen was considered to proceed to Co_3O_4 and the reaction of reduced tungsten with oxygen was considered to proceed to WO_6. Percentage (%) dispersion and percentage (%) reduction were calculated according to the method of Bartholomew and co-workers (*5, 35*).

Activity/selectivity measurements. CO hydrogenation activities and selectivities of the reduced catalysts were measured in a differential, fixed-bed flow reactor. Experiments were performed on 1 gram of catalyst at three different temperatures between 455 and 485 K. Low-activity catalysts were analyzed at higher temperatures. The reaction pressure was 1 atm with a molar H_2/CO ratio of 2. Reactant flowrates varied between 7 and 30 cm^3/min. Reaction products were fed through heated lines to an HP 5890A gas chromatograph for on-line analysis. Hydrocarbon products were separated in a 30-ft fused silica capillary column coated with SP 2100 and analyzed by an FID, while fixed gases were separated in a 6-ft Chromosorb 102 packed column and detected by a TCD. Response factors were determined using gas mixtures of known concentration. The activity/selectivity data were obtained under steady-state conditions (after at least 24 h run time) and at conversions of less than 10% (to maintain differential conditions). Two runs were made at each temperature and the average values for the two runs are reported.

RESULTS

Co/W Single Crystals

Activities. The CO hydrogenation activity and selectivity results for 0.75 ml Co/W(100) and 0.75 ml Co/W(110) are summarized in Table 1. The surfaces were tested in the range of 475–550 K, conditions typical for

TABLE 1

CO Hydrogenation Activity and Selectivity of 0.75 ml Co/W-(H_2/CO = 2.0, P = 750 Torr)

Crystal	Reaction temp. (K)	N_{CO}[a] ($\times 10^3$)	N_{CH_4}[b] ($\times 10^3$)	C_2 olefin fraction[c]	α[d]	E_{act}[e]
Co/W(100)	475	3.5	1.6	0.81	0.26	22.1
	475	4.8	2.7			
	500	10.4	5.7	0.86	0.21	
	500	15.0	7.3			
	525	33.4	18.2	0.75	0.19	
	525	42.5	17.3			
	550	82.2	49.3	0.83	0.18	
Co/W(110)	475	4.0	2.5	0.95		
	500	18.3	10.4	0.86		

[a] Carbon monoxide turnover frequency (molecules/site/s).
[b] Methane turnover frequency (molecules/site/s).
[c] C_2 olefin fraction = moles ethylene/(moles ethelene + moles ethane).
[d] C_1–C_4 Anderson–Schulz–Flory propagation probability.
[e] Activation energy for CO conversion (kcal/mol).

Fischer–Tropsch synthesis on cobalt. The 95% confidence limits on N_{CO} of Co/W(100) (obtained by pooling the standard deviations of the repeat runs) are: 2.4×10^{-3}–6.6×10^{-3} at 475 K, 8.3×10^{-3}–18.4×10^{-3} at 500 K, and 27.1×10^{-3}–51.4×10^{-3} at 525 K. Such wide confidence limits are not unusual for these difficult single crystal kinetic tests, especially with only one repeat run at each temperature.

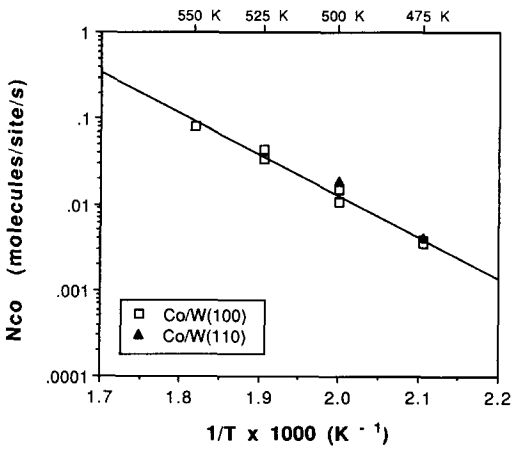

FIG. 1. Arrhenius plots for the steady-state CO turnover frequency of 0.75 ml Co/W(100) and 0.75 ml Co/W(110) at 750 Torr and H_2/CO = 2.

The Co/W(100) and Co/W(110) surfaces are similar in activity and selectivity. Figure 1 shows the Arrhenius plots for CO conversion on the two surfaces. The data points for Co/W(100) fit a straight line, giving an activation energy of 22.1 kcal/mol. The two data points for Co/W(110) fall nearly on the same line, and both values are within the 95% confidence limits of the Co/W(100) data. CO turnover frequencies of the clean (non-cobalt containing) tungsten crystals were found to be 2 orders of magnitude less than the cobalt overlayed crystals. Tungsten was chosen as the substrate metal partly because of its low activity for CO hydrogenation.

Selectivities. The C_2 olefin fraction falls between 0.75 and 0.95 for all of the tests. These olefin selectivities are quite high compared to those commonly found for supported cobalt catalysts (5). The Anderson–Schulz–Flory (ASF) propagation probabilities for Co/W(100) are very low compared to supported cobalt catalysts; however, they decrease with temperature as

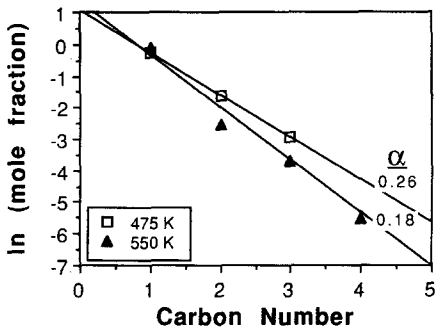

FIG. 2. Anderson–Schulz–Flory plots for 0.75 ml Co/W(100) at 475 and 550 K, 750 Torr, and H_2/CO = 2. α is the C_1–C_4 ASF propagation probability.

expected. Moreover, Fig. 2 shows that the ASF plots for Co/W(100) at 475 and 550 K are linear between C_1 and C_4. Because of the low propagation probabilities and low conversions, C_{5+} products were not detected.

AES spectra. Figure 3 compares the AES spectrum of the clean Co/W(100) surface (Spectrum (a)) with the AES spectrum obtained after 1 h of reaction at 475 K (Spectrum (b)). For Spectrum (b), the crystal was flashed to 600 K to remove molecularly adsorbed CO. The clean Co/W(100) surface has a Co(775 eV)/W(169 eV) ratio of about 0.17, which corresponds to 0.75 ml coverage

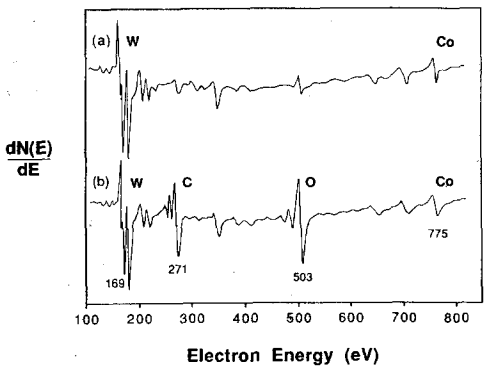

FIG. 3. AES spectra for 0.75 ml Co/W(100) (a) before reaction and (b) after 1 h of reaction at 475 K, 750 Torr, and H_2/CO = 2. Spectrum (b) was preceded by a 600 K anneal in vacuum to remove adsorbed CO.

TABLE 2

Carbon and Oxygen AES Ratios After Reaction[a]

Crystal[b]	Reaction temp. (K)	C(271 eV)/W(169 eV)	O(503 eV)/W(169 eV)
Co/W(100)	475	0.64	0.76
	500	0.71	0.49
	525	0.64	0.48
Co/W(110)	475	0.84	0.60
	500	0.63	0.72

[a] CO hydrogenation reaction performed at 750 Torr and H_2/CO = 2 for 1 h. AES spectrum obtained after a 600 K anneal under vacuum to remove molecularly adsorbed CO.

[b] Cobalt coverage was 0.75 ml.

of cobalt (*1*). The small C(271 eV) and O(503 eV) signals for this surface (Fig. 3a) are due to a small amount of molecularly adsorbed CO. After reaction, the C and O signals are very large, with a C(271 eV)/W(169 eV) ratio of 0.64 and an O(503 eV)/W(169 eV) ratio of 0.76. The ratios are measured versus tungsten instead of cobalt because of the weak cobalt signal. The lineshape of the C(271 eV) signal indicates that the adsorbed carbon is "carbidic" in nature, as opposed to "graphitic" carbon (*41*).

Table 2 lists the after reaction C/W and O/W AES ratios for Co/W(100) and Co/W(110) at each temperature. The AES spectra were taken after a 600 K anneal to remove molecularly adsorbed CO. The C/W and O/W ratios are quite high and are approximately equal. The reaction temperature and substrate geometry do not seem to affect the ratios. Because of the difficulty in differentiating between carbon and oxygen adsorbed on the cobalt overlayer and that adsorbed on exposed tungsten sites, no attempt was made to calculate the actual coverage of carbon and oxygen on the cobalt surfaces. In all cases, the C(271 eV) lineshape was characteristic of carbidic carbon.

Cobalt/Alumina Catalysts

Physical properties. Table 3 compares the physical properties of eight carbonyl-de-

TABLE 3

Physical Properties and CO Turnover Frequencies of the Carbonyl-Derived Alumina-Supported Catalysts Compared with Some Conventionally Prepared Catalysts

Catalyst[a]	Dehydroxylation temperature (K)	Metal loading (wt%)	Hydrogen uptake (μmol/g)	Dispersion[b] (%)	Reduction[c] (%)	N_{CO}[d] ($\times 10^3$) at 485 K
1% Co(923)	923	1.2	7	20	36	0,3
3% Co(923)	923	2.9	17	10	67	1.5
5% Co(923)	923	4.8	22	6	96	4.3
1% Co(1223)	1223	1.1	8	24	36	0.4
3% Co(1223)	1223	3.2	78	37	75	3.6
5% Co(1223)	1223	5.1	57	26	51	3.0
3% W(1223)	1223	2.5	11	110	15	0.01
Co/W(1223)	1223	2.2(Co) 2.0(W)	65	37[e] 110[e]	75[e] 15[e]	4.5
3% Co(conv)[f]	Conv. Prep.[g]	3	6	10	22	1.7
10% Co(conv)[f]	Conv. Prep.[g]	10	29	10	34	5.5

[a] Weight percentage of metal on alumina; dehydroxylation temperature of gamma alumina support is indicated in parenthesis for carbonyl-derived catalysts.

[b] Fraction of metal atoms exposed as determined from hydrogen adsorption; calculated according to Reuel and Bartholomew (*35*).

[c] Extent of reduction calculated from oxygen titration of reduced catalyst at 673 K assuming cobalt metal is oxidized to Co_3O_4 (*35*), and tungsten metal is oxidized to WO_6.

[d] Carbon monoxide turnover frequency (molecules/site/s) at 1 atm and $H_2/CO = 2$.

[e] Estimated. See Results section for explanation.

[f] Data taken from Ref. (*4*).

[g] Conventionally prepared cobalt/alumina catalysts. Prepared from aqueous nitrate impregnation, followed by calcination and reduction.

rived Co/alumina, W/alumina, and Co/W/alumina catalysts with those of two conventionally prepared Co/alumina catalysts. The catalysts' CO turnover frequencies at 485 K are included for comparison purposes (detailed activity results are in Table 4). The Co/W/alumina catalyst was prepared by sequentially depositing tungsten and then cobalt (by Soxhlet reflux) onto a 1223 K dehydroxylated (1223 DHD) support, followed by reduction at 623 K in hydrogen. This reduced Co/W catalyst was prepared as a supported analogue of the Co/W single crystal surfaces. The conventional catalysts were prepared by aqueous impregnation of cobalt nitrate followed by calcination and reduction. Data for these latter catalysts were taken from Reuel and Bartholomew (*4*).

For the 923 DHD catalysts, trends of increasing hydrogen uptake, increasing percentage reduction, increasing activity, and decreasing percentage dispersion with increasing metal loading are observed (see Table 3). None of these trends occurs for the 1223 DHD catalysts. The dehydroxylation temperature does not seem to affect the properties of the 1 wt% Co catalysts, but the 3% Co(1223) and 5% Co(1223) catalysts have significantly higher values of hydrogen uptake and percentage dispersion than their 923 DHD counterparts. The 3% W(1223) catalyst contains a significant fraction (0.15)

of reduced W metal with very high dispersion. Obviously, the result of 110% dispersion is not physically possible, but this value is within experimental error of unity dispersion.

Since it is not possible to differentiate the hydrogen uptakes of the cobalt and tungsten phases in the supported Co/W(1223) catalyst, values of percentage dispersion and percentage reduction could only be estimated. Assuming the 2.2 wt% cobalt phase to have 37% dispersion and 75% reduction (like the 3% Co(1223) catalyst) and the 2.0 wt% tungsten phase to have 110% dispersion and 15% reduction (like the 3% W(1223) catalyst), theoretical hydrogen and oxygen uptakes of 62 μmol/g and 215 μmol/g are calculated. The actual hydrogen uptake is 65 μmol/g and the actual oxygen uptake is 237 μmol/g. Accordingly, these assumptions are consistent with the data.

All of the carbonyl-derived cobalt catalysts have significantly higher extents of reduction than the conventionally prepared catalysts. While the dispersions of the 923 DHD catalysts are similar to those of the conventional catalysts, the dispersions of the 1223 DHD catalysts are much higher.

Activities. Table 4 lists the CO hydrogenation activity/selectivity results for the carbonyl-derived catalysts. It should be noted that the activity tests on the 1% Co(923), 1% Co(1223), and 3% W(1223) catalysts were performed at higher temperatures than the rest. Reported results are for steady-state conditions (after 24 h of reaction). Activities of the cobalt catalysts declined between 10 and 30% over the first 24 h, after which no further deactivation was observed. The 5% Co(923), 3% Co(1223), 5% Co(1223), and Co/W(1223) catalysts have very similar CO hydrogenation activities. The other cobalt catalysts are somewhat less active. The activity of the 3% W(1223) catalyst is 2 orders of magnitude less than that of the cobalt catalysts. Arrhenius plots are linear for all of the catalysts, and activation energies vary from 20.6 to 36.3 kcal/mol. Activation energies are higher for the 1223 DHD catalysts than for the 923 DHD catalysts.

Selectivities. The 923 DHD catalysts have CO_2 makes and olefin selectivities much higher than those of the 1223 DHD catalysts. ASF propagation probabilities are not affected by the dehydroxylation temperature. CO_2 makes, olefin selectivities, and ASF propagation probabilities all decrease with increasing reaction temperature. The reaction follows standard ASF kinetics for all of the catalysts. Figure 4 shows that the ASF plots for 5% Co(923) at 456 and 484 K are linear over the range of C_3–C_{13}.

DISCUSSION

Co/W Single Crystals

Structure and chemisorption. In a previous study (*1*), it was found that cobalt forms pseudomorphic monolayers on W(110) and W(100), which are thermally stable to 1300 K. The cobalt overlayers are geometrically strained with respect to bulk cobalt surfaces. The degree of strain is important for determining the effects of geometry or structure on the catalytic properties of cobalt. The pseudomorphic monolayer of Co/W(110) has an atomic density 21% less than Co(0001), while the pseudomorphic monolayer of Co/W(100) has an atomic density 45% less than Co(100). Thus, any effect of expanded geometry on the CO hydrogenation reaction would be more pronounced on the Co/W crystals than on bulk cobalt. The effect would also be larger on Co/W(100) than on Co/W(110). The cobalt monolayers are also electronically altered by the tungsten substrates, with net electronic donation from cobalt to tungsten for Co/W(110) and from tungsten to cobalt for Co/W(100).

The altered geometry and electronics of the surfaces change their chemisorptive properties, with two new binding states for hydrogen and two sites for CO dissociation. CO dissociates at 300 K on Co/W interfacial sites (found only on surfaces with submonolayer coverages of cobalt) and on the pseudomorphic monolayer of Co/W(100).

The 0.75 ml Co/W surfaces (which were tested for activity) thus both have enhanced CO dissociation ability, similar to that of

TABLE 4

CO Hydrogenation Activity and Selectivity of the Carbonyl-Derived Alumina-Supported Catalysts

Catalyst[a]	Reaction temperature (K)	N_{CO}[b] ($\times 10^3$)	E_{act}[c] (kcal/mol)	CO_2 make[d]	C_3–C_7 olefin make[e]	α[f]
1% Co(923)	498[g]	0.4	20.6	0.68	—	—
	513	0.9		0.56	—	—
	527	1.4		0.53	—	—
3% Co(923)	455	0.3	23.6	0.59	—	—
	469	0.6		0.32	0.88	0.55
	485	1.5		0.18	0.82	0.50
5% Co(923)	456	0.7	27.8	0.31	0.87	0.66
	470	1.7		0.15	0.76	0.58
	484	4.1		0.09	0.70	0.53
1% Co(1223)	496[g]	0.7	31.4	0.07	0.64	0.30
	513	2.4		0.07	0.46	0.22
	528	4.9		0.07	0.30	0.16
3% Co(1223)	456	0.6	27.6	0.10	0.45	0.57
	469	1.5		0.06	0.33	0.50
	485	3.6		0.06	0.35	0.48
5% Co(1223)	458	0.3	36.3	0.04	0.70	0.63
	471	0.9		0.04	0.59	0.56
	484	2.8		0.03	0.57	0.52
3% W(1223)	500[g]	0.015	—	0.00	—	—
	550	0.020		0.00	—	—
	620	0.027		0.00	—	—
Co/W(1223)	456	0.5	33.1	0.03	0.52	0.56
	470	1.5		0.03	0.37	0.53
	484	4.3		0.03	0.40	0.45

[a] Weight percentage of metal on alumina; dehydroxylation temperature of gamma alumina support is indicated in parenthesis for carbonyl-derived catalysts.

[b] Carbon monoxide turnover frequency (molecules/site/s) at 1 atm and $H_2/CO = 2$.

[c] Activation energy for CO conversion.

[d] Percentage carbon dioxide produced, based on a carbon atom balance.

[e] Mole percent olefins produced (moles C_3–C_7 olefins/(moles C_3–C_7 olefins + moles C_3–C_7 paraffins)).

[f] C_3–C_{13} Anderson–Schulz–Flory propagation probability.

[g] Higher reaction temperatures were necessary to observe measurable activity.

step sites of cobalt (*20*). The Co/W(100) surface has somewhat greater CO dissociation ability than that of the Co/W(110) surface. Since CO dissociation is a critical step in the CO hydrogenation reaction and has been demonstrated in the case of Ni to be the rate-determining step at low to moderate reaction temperatures (*42–45*), differences in activity for these surfaces relative to each other and to conventional cobalt surfaces might be expected at milder reaction conditions.

Activities. Unexpectedly, the steady-state CO hydrogenation activity of 0.75 ml Co/W(110) nearly matches the activity of 0.75 ml Co/W(100). While the amount of data for Co/W(110) is limited, both data points are within the 95% confidence limits of the better defined Co/W(100) results. The activity measured for the Co/W crystals is that of the cobalt sites, since background checks showed the tungsten crystals to have very low activity.

Since Co/W(100) has a very different ge-

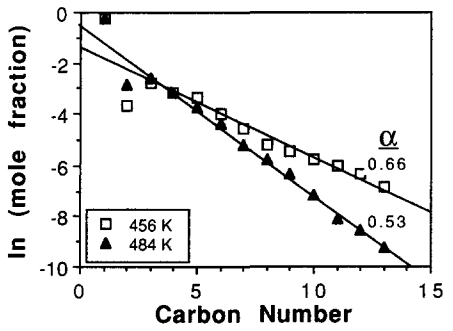

FIG. 4. Anderson–Schulz–Flory plots for 5% Co(923) at 456 and 484 K, 1 atm, and $H_2/CO = 2$. α is the C_3–C_{13} ASF propagation probability.

ometry and higher geometric strain than Co/W(110), the activity results suggest that initial geometry does not play a significant role in determining the steady-state activity of cobalt surfaces. This is very similar to results found for Ni (*13*), Ru (*14*), and Ni/W (*15*) single crystal surfaces. The structure insensitivity of CO hydrogenation on Co/W is somewhat surprising, since CO and H_2 chemisorption on the Co/W surfaces were quite different from those of bulk cobalt surfaces (*1*), and because CO dissociation has been shown to be structure sensitive on cobalt and nickel (*17–21*). The structure insensitivity of these surfaces may be explained by the "leveling" effect (*46*) of the relatively high carbon coverages on both steady-state surfaces. This effect is discussed in more detail in the subsection on AES Spectra.

A significant weakness in the argument for structure insensitivity of the Co/W surfaces is the fact that due to limitations in the experimental equipment, the Co geometry could not be determined during or after reaction. It is possible that the Co overlayers are not structurally stable under the high-temperature and pressure reaction conditions of CO hydrogenation and might reconstruct from their distinctly different surface geometries to highly similar geometries or form large Co crystallites. However, these Co overlayers were shown to be thermally stable to 1300 K in vacuum (*1*), indicating strong Co–W bonds in the Co/W pseudomorphic monolayer. Also, a significant amount of three-dimensional clustering would decrease the surface area of cobalt and decrease the crystal's activity. This decrease in activity was not observed, as the Co/W surfaces both have high activity for CO hydrogenation. Three-dimensional clustering of the Co during reaction would also be accompanied by a decrease in the Co/W AES ratio, but this did not occur, as can be seen in Fig. 3. This does not preclude the possibility of formation of very small Co crystallites (5–10 Å).

Another argument against a change in geometry during reaction can be found with the results for the CO hydrogenation and ethane hydrogenolysis reactions on Ni/W(110) and Ni/W(100) surfaces (*15*). While CO hydrogenation was found to be structure insensitive, the ethane hydrogenolysis reaction was found to be sensitive to the structure of Ni/W(110) and Ni/W(100), corroborating results found earlier on Ni(100) and Ni(111) (*12*). The Ni/W results would not be expected to so closely mimic the Ni single crystal results if significant changes in the Ni overlayer geometry occur during reaction. The Co/W surfaces are very similar in geometry and stability to the Ni/W surfaces (*1*).

Figure 5 compares the Arrhenius plot for *methane* formation on the Co/W surfaces with those found for other single crystal catalysts in the same temperature range. All results were determined under steady-state reaction conditions with H_2/CO ratios between 2 and 4, and pressures between 120 and 750 Torr. The agreement among the six systems in activity and activation energy are surprisingly good, especially between Co/W and Ni(100). Activation energies are 29.3, 18.4, 24.0, 23.7, 24.7, and 32.7 kcal/mol for polycrystalline Co (*31*), Ni/W (*15*), Rh foil (*47*), Co/W, Ni(100) (*13*), and Ru(100) (*14*), respectively. Thus, it appears that reaction specificity (variation in activity with the catalytic metal used (*2*)) effects are small for CO methanation on Group VIII metal single

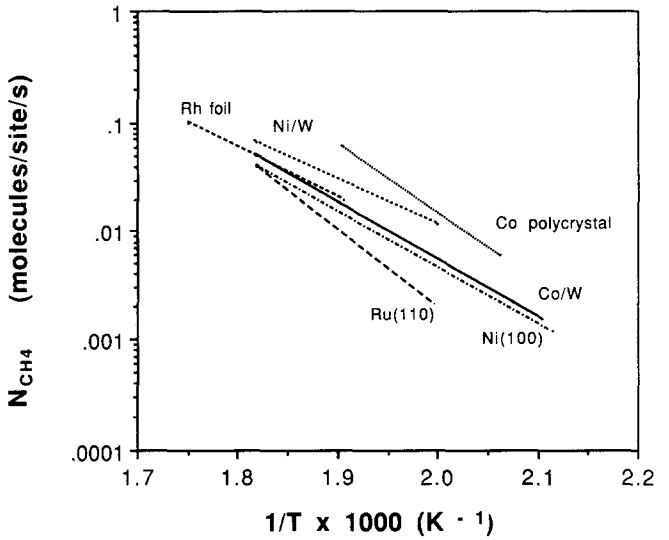

FIG. 5. Comparison of the Arrhenius plots for the steady-state CH_4 turnover frequency of polycrystalline CO, Ni/W, Rh foil, 0.75 ml Co/W, Ni(100), and Ru(110). Pressures varied from 120 to 750 Torr and H_2/CO ratios varied from 2 to 4. The polycrystalline Co, Ni/W, Rh foil, Ni(100), and Ru(110) plots were reproduced from Refs. (*31, 15, 47, 13, 14*), respectively.

crystals. Specificity is more important for methanation on supported metal catalysts (*2*), and is also more important for the selectivity to higher hydrocarbons. Reaction studies on iron foil (*48*) have found specific activities which are 1–2 orders of magnitude higher than the activity of the metals in Fig. 5. However, the iron activity was determined under initial conditions, and the iron was observed to extensively deactivate with time.

Selectivities. The olefin selectivity of the Co/W surfaces is high compared to commonly reported values for supported cobalt (compare Tables 1 and 4). This may result from the high carbon coverages of the surfaces (discussed in the subsection on AES Spectra). The olefin selectivity is believed to be related to the relative rate of the termination reactions for growing hydrocarbon chains, (i) β-hydrogen abstraction to produce α-olefins and (ii) hydrogenation to produce paraffins (*42, 43*). Since surface carbide is known to lower the hydrogen coverage of surfaces (*49*), high carbon coverage would favor olefin formation. High olefin selectivities were also found for Rh foil (*47*) and for Fe foil (*48*).

ASF propagation probabilities are expected to be high for carbon-covered surfaces, but the opposite seems to be true for Co/W. Propagation probabilities for supported cobalt under the same conditions (compare Tables 1 and 4) are a factor of two or more higher than those found for Co/W. However, α's have been commonly found to be very low for CO hydrogenation on single or polycrystalline surfaces. In the Fischer–Tropsch temperature range, polycrystalline Co (*31*), Rh foil (*47*), and Fe foil (*48*) all have α's of 0.30 or less. The low propagation probabilities of single crystal catalysts relative to supported catalysts are difficult to explain, but occur for all of the metals tested so far. One important difference between supported metals and well-defined surfaces that might explain this phenomenon is the presence in the former (absence in the latter) of pores which are readily filled with hydrocarbon liquids during reaction. The slower transport through the liquid pores and potential for readsorp-

tion could increase the propagation probability.

AES spectra. The AES spectra establish the surface cleanliness of the Co/W surfaces before reaction and show no contamination after reaction, except for carbon and oxygen reaction intermediates. In all cases, the adsorbed carbon is clearly carbidic in nature, and no graphite is formed at temperatures of 550 K or below. Graphite formation has been found during CO hydrogenation on other single crystal surfaces, but only above 650 K on Ni(100) (*50*), above 600 K on Ru(110) (*51*), and above 575 K on Fe foil (*48*). At lower temperatures the carbon AES signals are carbidic, and the C/Ni ratio of Ni(100) and the C/Ru ratio of Ru(110) are found to be around 0.10. The C/Co ratio of polycrystalline Co (*31*) has been reported to be about 0.2–0.5 following reaction. The C/W ratios of 0.63 or above found for Co/W are significantly higher, indicating a higher steady-state surface carbide level on cobalt. This may be the result of the enhanced CO dissociation ability of the Co overlayers.

It is interesting that this enhanced CO dissociation ability increases the surface carbide level, but does not seem to affect the steady-state activity. This same result could be expected for cobalt surfaces with high concentrations of low coordination step and kink sites. Somorjai and Carrazza (*46*) have suggested that while the bonding of molecules to surfaces is almost always structure sensitive, high coverages of adsorbed species can mask or "level" the surface structure of the catalyst, thus weakening reactant–surface interactions and making reactions on the surface structure insensitive.

The high oxygen coverages for Co/W are unique, as no oxygen AES signal is observed after reaction for Ni(100) (*41*) and Rh foil (*47*). The retention of oxygen on the Co/W surface may result because of tungsten's affinity for oxygen, especially since the observed oxygen coverage on polycrystalline cobalt after reaction was low (*31*). In fact, the tungsten substrate may be partially oxidizing or carbiding during reaction, contributing to the large oxygen and carbon signals in the AES spectra. More quantitative XPS studies would have to be performed on the Co/W surfaces after reaction to determine how much of the oxygen and carbon are bonded to Co or W. However, it is reasonable to believe that a significant portion of the carbon is bonded to the Co overlayer, since this has been established as the active phase for CO hydrogenation, and since C/Co ratios are 0.2–0.5 on polycrystalline cobalt (*31*).

Co/Alumina Catalysts

Physical properties. Co/alumina catalysts prepared by conventional aqueous impregnation with weight loadings below 10% typically have percentage dispersions below 15% and percentage reductions below 35% (*4, 5*). A trend of decreasing specific CO hydrogenation activity with decreasing metal loading and increasing dispersion is observed for these conventionally prepared catalysts. The Co/alumina catalysts of this study were prepared by nonaqueous decomposition of carbonyls on a dehydroxylated support in an attempt to obtain catalysts of higher dispersion and higher extent of reduction. The objective was to determine if this same activity trend would be obtained on highly dispersed, highly reduced Co/Al_2O_3 catalysts. It was previously reported (*36–38, 40*) that carbonyl-derived catalysts have higher percentage dispersion and percentage reduction than their conventionally prepared counterparts. Burwell (*37*) and Brenner and Hucul (*38*) have shown that hydroxyl groups on the surface of alumina supports act as adsorption sites for metal carbonyls (resulting in highly dispersed catalysts), but oxidize the metal during-decomposition. However, decomposing metal carbonyls on *dehydroxylated* aluminas can produce supported catalysts which are both low-valent and well-dispersed.

The data in Table 3 show that the carbonyl-derived Co/Al_2O_3 catalysts are all highly reduced. Even the 1% Co catalysts

have higher extents of reduction than the conventionally prepared 10% Co catalyst. The increased extent of reduction of the carbonyl-derived catalysts is undoubtedly the result of the preparation method, which employs a precursor with the cobalt atoms already in the zero-valent state, and an alumina support with low concentration of surface hydroxyl groups. The 1223 DHD alumina is nearly but not completely dehydroxylated, retaining only about 1% of the hydroxyl groups originally present on the hydroxylated support (*37*). Some surface area loss and δ-alumina formation can be expected at this temperature, but the loss of area was not catastrophic, considering the high cobalt dispersions and high hydrogen uptakes of the 1223 DHD catalysts.

The dehydroxylation temperature seems to principally affect the catalyst dispersion. That is, the 1223 DHD catalysts have significantly higher dispersions than their 923 DHD counterparts. This suggests that $Co_4(CO)_{12}$ interacts strongly with the sites created by dehydroxylating the alumina surface. Burwell (*37*) speculates that Lewis acid–Lewis base pair sites created by dehydroxylation adsorb metal carbonyls, which then form highly dispersed zero-valent metal sites upon decomposition of the carbonyl. The fact that increasing the dehydroxylation temperature did not significantly affect the physical properties of the 1% Co catalysts suggests that there are enough Lewis acid–Lewis base pair sites on the 923 DHD alumina to accommodate 1% Co.

The high extent of dehydroxylation of the 1223 DHD alumina also results in a 3% W/alumina catalyst with unity dispersion and a significant extent of reduction. Tungsten interacts strongly with alumina supports and it was previously thought that reduced tungsten could not be produced on alumina. The fact that the 3% W(1223) catalyst takes up both hydrogen and oxygen is a strong indication that at least some of the tungsten is zero-valent. This catalyst is similar to previously produced Mo/alumina and W/alumina catalysts (*37, 38*). The supported tungsten apparently does not interact much with the cobalt phase on the Co/W(1223) catalyst, since the estimated percentage dispersion and percentage reduction of the two phases are similar to those of the 3% Co(1223) and 3% W(1223) catalysts.

The 1223 DHD cobalt catalysts, which have high percentage dispersion *combined* with high percentage reduction, have very high surface areas of the active metallic phase, as demonstrated by their high hydrogen uptakes. This high surface area combined with these catalysts' high specific activities and activity stability result in high steady-state rates on a weight basis. High weight basis activity is unusual for catalysts of such low weight loading.

Activities. The highly reduced 5% Co(923), 3% Co(1223), and Co/W(1223) catalysts have very similar Fischer–Tropsch activities, even though their dispersions vary from 6 to 37%. The 5% Co(1223) catalyst has just slightly lower activity but a high activation energy, so a case could be made that its activity is within experimental error of the other three (see Table 3). The activities and activation energies of these catalysts are quite similar to values reported in the literature for both conventional (*52*) and carbonyl-derived (*36, 53*) cobalt catalysts. The 1% Co catalysts and the 3% Co(923) catalyst clearly have significantly lower activity than the other four carbonyl-derived catalysts. A crucial question (which is addressed in the Comparison section) is, Why do these catalysts have lower specific activity?

The activity of the 3% W(1223) catalyst is 2 orders of magnitude less than that of the cobalt containing catalysts, even though 15% of the tungsten is in the reduced form. The same result was found for the W single crystals compared to the Co/W crystals, providing further evidence that tungsten is inactive (compared to cobalt) for the CO hydrogenation reaction.

The carbonyl-derived catalysts deactivate less than 30% over the first 24 h and

then maintain that activity thereafter. This high activity–stability is very similar to those of conventionally prepared cobalt catalysts.

Selectivities. The principle difference in selectivity among the supported catalysts is the large decrease in the CO_2 make when increasing the dehydroxylation temperature from 923 to 1223 K. CO_2 is produced by the reaction of CO_{ads} with O_{ads}, or by the water gas shift reaction. It is not clear whether this takes place on the metallic phase or on oxidic phases of the supported catalysts, but the extent of this reaction seems to be affected most by the chemical nature of the support, not the percentage dispersion or percentage reduction of the cobalt. The lower olefin makes of the 1223 DHD catalysts might also be considered a support effect.

Propagation probabilities are very similar to those of conventionally prepared cobalt catalysts, in contrast to those of the Co/W crystals. The α's are not affected by the dehydroxylation temperature. Figure 4 shows that the hydrocarbon selectivities of the supported carbonyl-derived catalyst conform to ASF theory, contrary to previous reports (*54, 55*). This phenomenon is discussed in more detail elsewhere (*36*).

Comparison of the Single Crystal and Supported Catalyst Results

Arrhenius plot. Figure 6 compares the Arrhenius behavior of four of the supported Co/alumina catalysts with those of the Co/W crystals. The supported catalysts vary in dispersion from 6 to 37%, and the 10% Co catalyst is conventionally prepared. The activities and activation energies of these highly reduced supported catalysts compare remarkably well with those of the Co/W single crystals, especially considering the differences in the batch and flow reactor systems used. The figure is similar to an Arrhenius plot comparison for CO hydrogenation on single crystal and supported nickel catalysts (*13*).

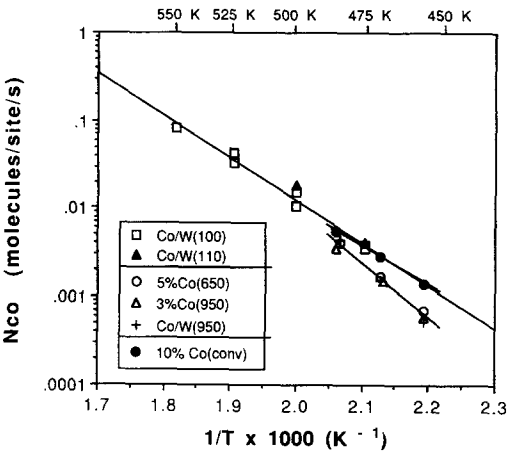

FIG. 6. Comparison of the Arrhenius plots for the steady-state CO turnover frequency of the 0.75 ml Co/W crystals with plots for four Co/alumina catalysts. Reaction conditions were 1 atm and $H_2/CO = 2$. The Co/alumina catalysts were carbonyl-derived, except for the 10% Co(conv) catalyst, which was prepared by aqueous impregnation (*4*).

Effects of percentage dispersion and percentage reduction. Figure 7 is a plot of the activity of the catalysts at 485 K versus their percentage dispersion. The results for the Co/W crystals and for polycrystalline Co are included. The cobalt monolayers on the W crystals are considered to be 100% dispersed while the polycrystalline surface has a dispersion approaching 0%.

As shown by the horizontal line spanning the full range of dispersion (0–100%), the activities of four of the carbonyl-derived catalysts of high percentage reduction and moderate loading (3–5%) are the same within experimental error as those of the 10% Co(conventional preparation) catalyst, the Co/W crystals, and the Co polycrystal. Thus, the rate of the CO hydrogenation is independent of dispersion on well-reduced cobalt surfaces. Data for well-reduced, carbonyl-derived Fe/alumina catalysts also show no change in activity with dispersion (*30*).

On the other hand, there is a trend of decreasing activity with increasing dispersion for some of the 1 and 3 wt% Co/alumina catalysts (the dashed line), similar to that

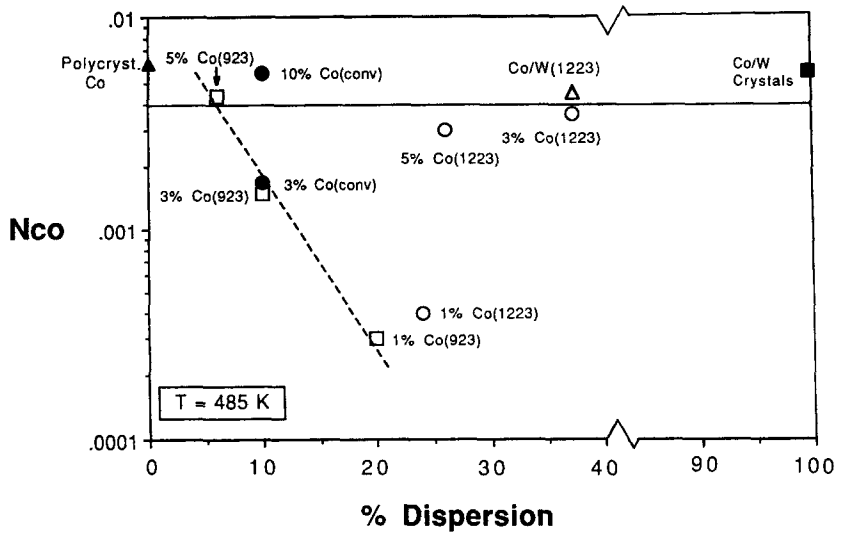

FIG. 7. Carbon monoxide turnover frequency (485 K, 1 atm, $H_2/CO = 2$) versus % dispersion of the Co/alumina catalysts. Carbonyl-derived catalysts have open symbols. The turnover frequencies of Co/W single crystals and of polycrystalline Co are included for comparison.

of conventionally prepared catalysts. This result may relate to reduction and/or support effects. One possibility for the lower activity of these catalysts is contamination by or interaction with some oxidic phase on the supported catalyst (*24, 30*). This idea is supported by Fig. 8 which shows a trend of increasing activity for the carbonyl-derived catalysts with increasing percentage reduction of the cobalt. The 3 and 5 wt% Co 1223 DHD catalysts have very high dispersions but also have high specific activities (Figure 7), suggesting that the activities of moderately loaded carbonyl-derived catalysts prepared with this high dehydroxylation temperature are not lowered by support or unreduced oxide contaminants.

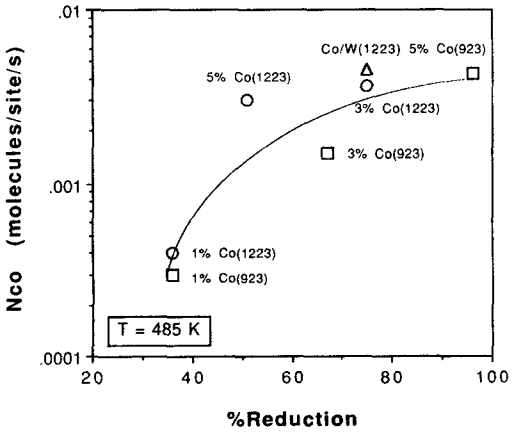

FIG. 8. Carbon monoxide turnover frequency (485 K, 1 atm, $H_2/CO = 2$) versus % reduction of the carbonyl-derived Co/alumina catalysts.

Comparison to Previous Theories

In the Introduction section we listed three theories which have been suggested to explain the variations in activity with dispersion for supported CO hydrogenation catalysts. The theories were primary structure sensitivity, secondary structure sensitivity, and metal support interactions. The results of this study show that the activity of well-reduced cobalt is independent of dispersion; this combined with the data for Co/W and for other single crystal systems (*13–15*) suggests that the CO hydrogenation reaction is primary structure *in*sensitive.

Secondary structure sensitive theories suggest that the enhanced CO dissociation ability of low coordination sites causes poi-

soning by graphite or by a high surface carbide level. The Co/W surfaces have enhanced CO dissociation ability, but do not form graphite under reaction conditions. A high surface carbide level does form, but this does not produce a low activity catalyst. Thus, the results of this study are not consistent with secondary structure sensitive theories.

The trends of increasing activity with increasing percentage reduction and increasing dehydroxylation temperature suggest that some of the metal sites on the less active, poorly reduced catalysts are interacting with a metal oxide phase or with the support. A key to isolating this effect may be found with the 3% Co(1223), 5% Co(1223), and Co/W(1223) catalysts, which have highly dispersed metal clusters, but do not show this interaction. The CO_2 and olefin makes of these catalysts are much lower than those of the less active catalysts. Thus, the chemical nature of the support surface, not the metal crystallite size, appears to be the controlling factor in determining the activity and selectivity of these supported cobalt catalysts.

Temperature-programmed surface reaction (TPSR) studies are currently being performed on the carbonyl-derived catalysts to investigate this phenomenon. TPSR studies on conventionally prepared catalysts (*25–27*) have shown that there are two sites or reaction states for CO hydrogenation, and that the less active of these states may result from participation by the support. A higher relative abundance of this less active state could account for the lower activity of the less active catalysts. Moreover, recent Moessbauer and TPD studies (*28, 29*) of a poorly reduced, 1% Co/Al_2O_3 catalyst indicate that electronic and adsorption properties of the tiny metal clusters in these catalysts are greatly changed due to interaction with the support.

SUMMARY

(1) Steady-state CO hydrogenation activities of 0.75 ml Co/W(110) and 0.75 ml Co/W(100) are the same within experimental error. The activity and activation energy of these highly strained cobalt overlayers compare favorably with those of the highly active Co/alumina catalysts. Thus, surface geometry does not appear to play a significant role in determining the steady-state activity of cobalt surfaces.

(2) The methanation activity of the Co/W crystals is similar to that found for various crystalline surfaces of Co, Ni, Rh, and Ru.

(3) Co/W surfaces have higher selectivity for olefins and lower ASF propagation probabilities than supported Co catalysts.

(4) The after-reaction Co/W surfaces have high coverages of both carbon and oxygen. The carbon AES lineshapes are characteristic of carbidic carbon. No graphite forms under low temperature reaction conditions.

(5) The carbonyl-derived Co/alumina catalysts have higher percentage reduction than similar conventionally prepared catalysts, but have similar activity stability.

(6) Increasing the dehydroxylation temperature of the alumina from 923 to 1223 K dramatically increases the percentage dispersion and decreases the CO_2 and olefin selectivities. This increase in percentage dispersion does not decrease the activity of the catalysts.

(7) Changes in the specific activity and selectivity of the carbonyl-derived catalysts are more closely related to the percentage reduction and the support dehydroxylation temperature than to the percentage dispersion. Indeed, the specific activity of well-reduced cobalt catalysts is independent of dispersion over the full range of dispersion (0–100%). Thus, the chemical nature of the support surface appears to be the controlling factor in determining the activity and selectivity of supported cobalt catalysts.

ACKNOWLEDGMENTS

The authors acknowledge with pleasure the support of this work by the Department of Energy, Office of Basic Energy Sciences, Division of Chemical Sciences. The authors also gratefully acknowledge the

technical assistance of Mr. Richard Jones and Mr. Ray Helvy.

REFERENCES

1. Johnson, B. G., Berlowitz, P. J., Goodman, D. W., and Bartholomew, C. H., *Surf. Sci.* **217,** 13 (1989).
2. Boudart, M., and McDonald, M. A., *J. Phys. Chem.* **88,** 2185 (1984).
3. Kellner, C. S., and Bell, A. T., *J. Catal.* **75,** 251 (1982).
4. Reuel, R. C., and Bartholomew, C. H., *J. Catal.* **85,** 78 (1984).
5. Fu, L., and Bartholomew, C. H., *J. Catal.* **92,** 376 (1985).
6. Jones, V. K., Neubauer, L. R., and Bartholomew, C. H., *J. Phys. Chem.* **90,** 4832 (1986).
7. Jung, H. J., Walker, P. L., Jr., and Vannice, M. A., *J. Catal.* **75,** 416 (1982).
8. Bartholomew, C. H., Pannell, R. B., and Butler, J. L., *J. Catal.* **65,** 335 (1980).
9. Van Hardeveld, R., and Hartog, F., *Adv. Catal.* **22,** 75 (1972).
10. Bonzel, H. P., and Krebs, H. J., *Surf. Sci.* **117,** 639 (1982).
11. Spencer, N. D., Schoonmaker, R. C., and Somorjai, G. A., *J. Catal.* **74,** 129 (1982).
12. Goodman, D. W., *Surf. Sci.* **123,** L679 (1982).
13. Kelley, R. D., and Goodman, D. W., *Surf. Sci.* **123,** L743 (1982).
14. Kelley, R. D., and Goodman, D. W., *Amer. Chem. Soc. Div. Fuel Chem. Prep. Pap.* **25**(2), 43 (1980).
15. Greenlief, C. M., Berlowitz, P. J., Goodman, D. W., and White, J. M., *J. Phys. Chem.* **91,** 6669 (1987).
16. Manogue, W. H., and Katzer, J. R., *J. Catal.* **32,** 166 (1974).
17. Erley, W., and Wagner, H., *Surf. Sci.* **74,** 333 (1978).
18. Erley, W., Ibach, H., Lehwald, S., and Wagner, H., *Surf. Sci.* **83,** 585 (1979).
19. Murayama, Z., Kojima, I., Miyazaki, E., and Yasumori, I., *Surf. Sci.* **118,** L281 (1982).
20. Prior, K. A., Schwaha, K., and Lambert, R. M., *Surf. Sci.* **77,** 193 (1978).
21. Papp, H., *Surf. Sci.* **149,** 460 (1985).
22. Caracciolo, R., and Schmidt, L. D., *Appl. Surf. Sci.* **25,** 95 (1986).
23. Lee, C., Schmidt, L. D., Moulder, J. F., and Rusch, T. W., *J. Catal.* **99,** 472 (1986).
24. Bartholomew, C. H., *in* "Hydrogen Effects in Catalysis" (Z. Paal and P. G. Menon, Eds.), Chaps. 5 and 20. Elsevier, Amsterdam, 1988.
25. Lee, W. H., and Bartholomew, C. H., *J. Catal.* **120,** 256 (1989).
26. Glugla, P. G., Bailey, K. M., and Falconer, J. L., *J. Phys. Chem.* **92,** 4474 (1988); *J Catal.* **115,** 24 (1989); Sen, B., and Falconer, J. L., *J. Catal.* **113,** 444 (1988).
27. Huang, Y. J., and Schwarz, J. A., *Appl. Catal.* **30,** 239 (1987); **32,** 45 (1987).
28. Lee, W. H., and Bartholomew, C. H., in preparation, 1990.
29. Neubauer, L. R., and Bartholomew, C. H., in preparation, 1990.
30. Rameswaran, M., and Bartholomew, C. H., *J. Catal.* **117,** 218 (1989).
31. Bartholomew, C. H., Greenlief, C. M., Berlowitz, P. J., Johnson, B. G., and Goodman, D. W., in preparation, 1990.
32. Berlowitz, P. J., and Goodman, D. W., *Surf. Sci.* **187,** 463 (1987).
33. Berlowitz, P. J., and Shinn, N. D., *Surf. Sci.* **209,** 345 (1989).
34. Berlowitz, P. J., and Goodman, D. W., *Langmuir* **4,** 1091 (1988).
35. Reuel, R. C., and Bartholomew, C. H., *J. Catal.* **85,** 63 (1984).
36. Johnson, B. G., Rameswaran, M., Patil, M. D., Muralidhar, G., and Bartholomew, C. H., *Catal. Today* **6,** 81 (1989).
37. Burwell, R. L., *J. Catal.* **86,** 301 (1984).
38. Brenner, A., and Hucul, D. A., *J. Catal.* **61,** 216 (1980).
39. Kay, B. D., Peden, C. H. F., and Goodman, D. W., *Phys. Rev. B* **34,** 817 (1986).
40. Phillips, J., and Dumesic, J. A., *Appl. Catal.* **9,** 1 (1984).
41. Goodman, D. W., Kelley, R. D., Madey, T. E., and Yates, J. T., Jr., *J. Catal.* **63,** 226 (1980).
42. Biloen, P., and Sachtler, W. M. H., *Adv. Catal.* **30,** 165 (1981).
43. Bell, A. T., *Catal. Rev. Sci. Eng.* **23,** 203 (1981).
44. Goodman, D. W., *Acc. Chem. Res.* **17,** 194 (1984); *Ann. Rev. Phys. Chem.* **37,** 425 (1986).
45. Sughrue, E. L. and Bartholomew, C. H., *Appl. Catal.* **2,** 239 (1982).
46. Somorjai, G. A., and Carrazza, J., *Ind. Eng. Chem. Fundam.* **25,** 63 (1986).
47. Sexton, B. A., and Somorjai, G. A., *J. Catal.* **46,** 167 (1977).
48. Krebs, H. J., Bonzel, H. P., and Gafner, G., *Surf. Sci.* **88,** 269 (1979).
49. Kiskinova, M., and Goodman, D. W., *Surf. Sci.* **109,** L555 (1981).
50. Goodman, D. W., Kelley, R. D., Madey, T. E., and White, J. M., *J. Catal.* **64,** 479 (1980).
51. Goodman, D. W., and White, J. M., *Surf. Sci.* **90,** L201 (1979).
52. Fernandez-Morales, I., Guerrero-Ruiz, A., Lopez-Garzon, F. J., Rodriguez-Ramos, I., and Moreno-Castilla, C., *Appl. Catal.* **14,** 159 (1985).
53. Chen, A. A., Kaminsky, M., Geoffroy, G. L., and Vannice, M. A., *J. Phys. Chem.* **90,** 4810 (1986).
54. Vanhove, D., Zhuyong, Z., Makambo, L., and Blanchard, M., *Appl. Catal.* **9,** 327 (1984).
55. Commereuc, D., Chauvin, Y., Hugues, F., Basset, J. M., and Olivier, D., *Chem. Soc. Commun.*, 154 (1979).